# Application of piezoelectric composites to control operation of a gas foil bearing – prototype design and testing

# A Martowicz<sup>1\*</sup>, P Zdziebko<sup>1</sup>, J Roemer<sup>1</sup>, G Zywica<sup>2</sup>, P Baginski<sup>2</sup>, A Andrearczyk<sup>2</sup>

- 1. AGH University of Science and Technology, Department of Robotics and Mechatronics, al. Mickiewicza 30, 30-059 Krakow, Poland
  - 2. Institute of Fluid-Flow Machinery, Polish Academy of Sciences, Department of Turbine Dynamics and Diagnostics, Fiszera 14 str., 80-231 Gdansk, Poland

#### **ABSTRACT**

Essential parts of rotating machineries are supporting nodes, i.e., bearing systems. They assure required rotational degrees of freedom and feature desired load carrying capacity. Following the specificity of a technical solution considered, various types of bearings may be taken into account to effectively address the requirements regarding the speed and load. Specifically, gas foil bearings (GFB) are used in high-speed and lightly-loaded rotating machineries, e.g., auxiliary power units. In fact, they can operate up to several hundreds of thousands rpm, also for a wide temperature range. The current work reports an application of piezoelectric composites to control operation of a GFB. The authors present the developed bearing's prototype installation which is equipped with a specialized multifunctional structural component that advantageously allows to both characterize GFB's operational parameters and modify them. The experimental results confirm the usability of the proposed actively-controlled configuration of a GFB.

## 1. INTRODUCTION - GAS FOIL BEARINGS AND SMART GAS FOIL BEARINGS

High-speed rotating machineries require unique technical solutions to be implemented to address the specific operational conditions. One of the adequate choice regarding the type of the suspension nodes are gas foil bearings (GFB) [1,2]. These bearings can be used at very high rotational speed, i.e., up to several hundreds of thousands rpm, also for a wide temperature range [3,4,5]. Figure 1 shows the cross-sectional view of a typical radial GFB.

The structural part of the GFB's suspension layer is composed of a set of thin metallic top and bump foils made of an superalloy, e.g., Inconel 625. Complementarily, a several-micrometer-thin gaseous film composes a fluidic component of the suspension layer. During run-up stage of operation, due to the hydrodynamic action, an air film is developed in a GFB. Consequently, the shaft's journal elevates over the bearing's foils and then the system continues contactless high-speed operation. It is worth mentioning that, even though GFBs can work at high ambient temperatures, they require thermal control to maintain proper mechanical properties, including the desired capability of load carrying. Excessive temperature gradients observed within the surface of the bearing's foils may cause significant thermal expansions and finally a damage of the bearing [7,8,9].

<sup>\*</sup>Corresponding Author: adam.martowicz@agh.edu.pl

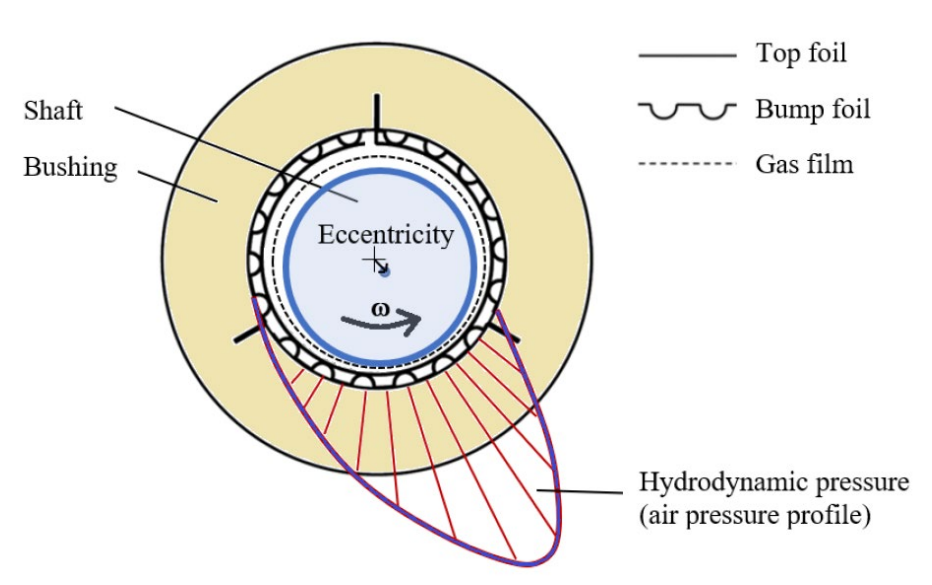


Figure 1: Cross-sectional view of a radial GFB [6].

The perspective of GFB's structural modifications, including introduction of various types of smart materials to enhance the operational properties of the considered bearings is under continuous investigation. Nowadays, both passive and active solutions are known and successfully implemented. Amongst others, the following structural modifications are considered to improve and control the elasto-damping characteristics of GFBs:

- substitution of bump foils with springs made of shape memory alloys (SMA) [10]; The approach allows for an active control of the GFB's elasto-damping properties with thermal excitation:
- application of piezoelectric transducers, e.g., piezoelectric composites macro fiber composites (MFC), to the GFB's foils [11,12,13]; The solution provides the means for fast modification of the bearing's operational properties via precise change of the foils' geometry;
- application of radially oriented piezoceramic (PZT) stacks installed in the GFB's bushing [14]; The approach enables fast and precise control of the clearance and preload;
- application of circumferentially oriented PZT actuators cooperating with mechanical amplifiers to control the GFB's clearance and preload [15,16,17];
- hybrid construction of a bearing composed with a classical ball bearing and a GFB [18];
   The unique solution is equipped with two different types of electromechanical actuators: electromagnetic coils and PZTs;

Various topology, geometric and size modifications are taken into account to improve the GFB's performance. The considered changes may affect both the bushing and the supporting foils. As briefly reported above, the desired enhancement of the bearing's properties may be achieved via applications of smart materials – providing solutions of smart GFBs. A comprehensive overview on the GFB's structural modifications and the caused effects regarding the bearing's behavior is provided in [6].

In the current paper, the authors describe an application of piezoelectric composites MFC to control operation of a GFB, that makes a reference to the works [11,12,13]. Worth highlighting here is that various composite (multi-material) structures are widely used in multiphysics applications to take an advantage of their useful active and passive capabilities (functions): e.g., withstanding the blast and impact loading [19,20,21], control vibrational and damping properties [22] and performing load identification via characterization of the electrical properties [23].

In the present study, specifically, the newly-designed and manufactured specialized multifunctional top foil is used to: (a) characterize the selected GFB's operational parameters, i.e., temperature and top foil's strain via integrated thermocouples and strain gauges, and (b) modify the bearing's behavior making use of the piezoelectric transducers.

The work is composed with 4 sections. After present introductory Section 1, that is dedicated to an overview on GFBs and the idea of a smart GFB, Section 2 presents the developed bearing's prototype installation equipped with piezoelectric transducers. In Section 3, the authors report the results of the conducted experiments, followed by a discussion on the performance of the examined technical solution. Summary and final conclusions are addressed in final Section 4.

## 2. PROTOTYPE OF A GAS FOIL BEARING EQUIPPED WITH PIEZOELECTRIC COMPOSITES

According to the assumed scope of the current work, the authors created a prototype installation of a smart GFB, making use of a novel configuration of the specialized top foil that is presented in Figure 2.

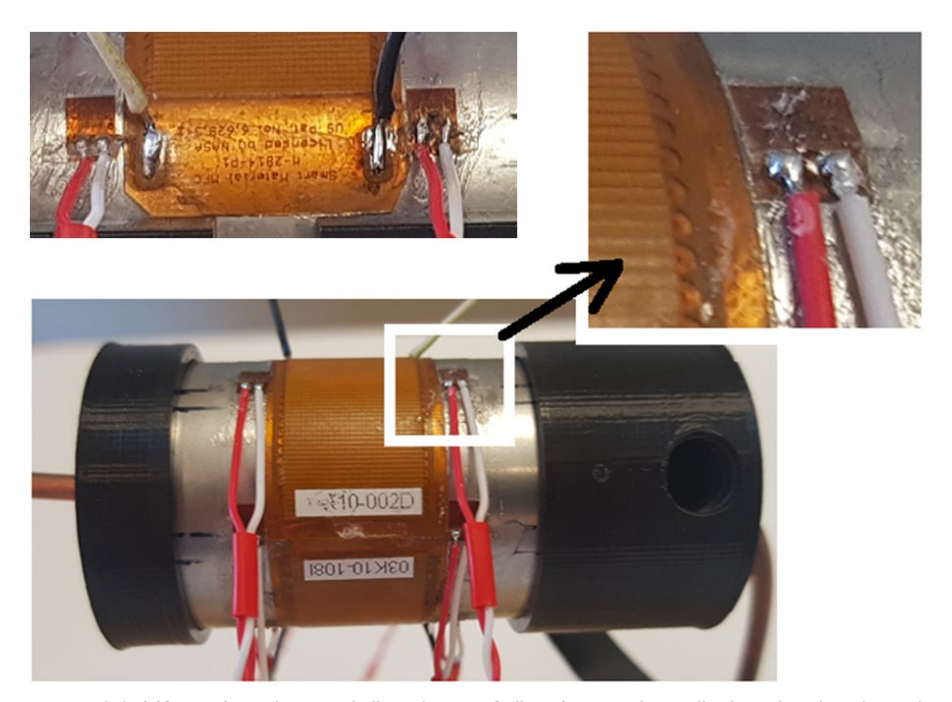


Figure 2: Multifunctional specialized top foil prior to installation in the bearings' bushing and welding of thermocouples. Close-up views show a strain gauge as well as soldering pads and electrodes of the two piezoelectric composite MFC.

Figure 3 presents an assembly of the spool-shaped bushing. The circumferentially and axially distributed openings allow for guidance of the sensor wires. A complete prototype installation of the tested GFB is shown in Figure 4. During experiments a floating configuration was used to provide preliminary results. In this case the shaft's journal supports the bearing. The air film is generated on top of the shaft and makes the GFB elevating, contrarily to the bearings' standard operational case when the shaft elevates over the top foil.



Figure 3: Assembly of the spool-shaped bushing tierces held with flanges – before installation of the specialized top foil.

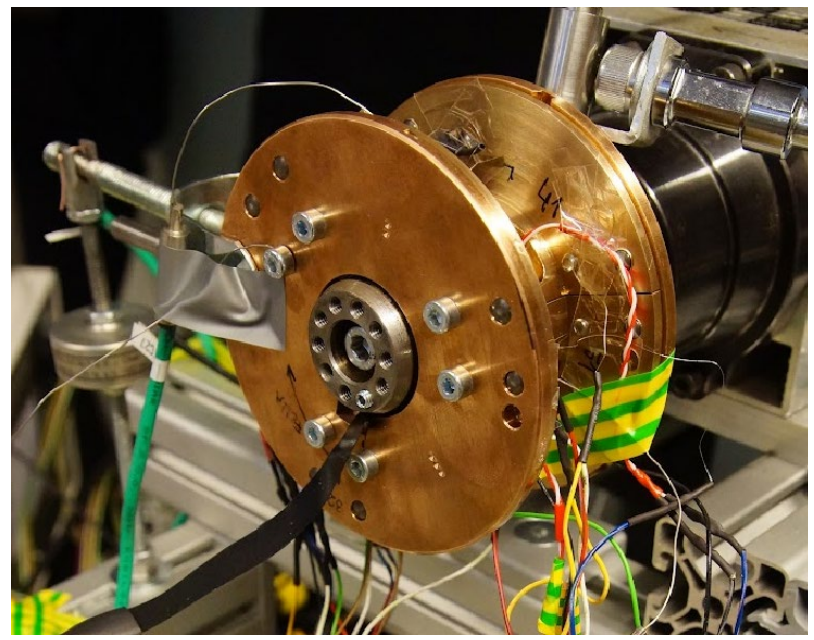


Figure 4: Assembled smart GFB during experimental tests.

In the examined GFB, the specialized top foil simultaneously operates as a sensor and an actuator that stands for the novelty of the proposed solution. Specifically, the thermocouples that are integrated with the top foil allow for temperature readings within the region where the air film develops. Similarly, the circumferentially and axially distributed strain gauges provide the data on the top foil's deformation that may be eventually used to track the cross-sectional shape evolution for the gaseous layer present above the shaft's journal. More details on the concept of measuring top foil installed in a GFB are presented in [24].

To perform electrically-activated modification of the top foil's shape, the authors used two MFC piezoelectric transducers M-2814-P1, manufactured by the company Smart Material. The characteristics of the applied transducers are specified in [25]. The most important ones are provided in Table 1.

Table 1: Properties of the used MFCs - M-2814-P1.

#### Parameter / feature Value / description Dominating piezoelectric effect d33 – parallel directions of electric field and deformation Electrode topology Comb-shaped, MFC P1-Orientation of piezoelectric Transverse orientation with respect to the electrodes fibers **Dimensions** Overall: 38mm x 20mm x 0.3mm (length x width x thickness) Active area: 28mm x 14mm Capacitance 1.9nF + /-20%146N -0% / +20% Blocking force Operating voltage -500V to 1500V Piezoelectric constant 400pC/N for d33-effect along fibers 30.34GPa (along fibers) / 15.86GPa (along electrodes) Tensile moduli Volume density $5.44 \text{ g/cm}^3$

The overall characteristics for piezoelectric transducers, including multiphysics nature of operation and multidomain constitutive relations, are discussed in [26]. Due to the specific inplane alternating distribution of electric potentials applied for the case of d33-effect, the used MFCs act as interdigital transducers (IDT) with the comb-shaped electrodes' pattern [27].

The authors of the current study intentionally chose MFCs to control operation of the GFB due to their high flexibility, apart from the piezoelectric materials' typical capability of precise change of the electrically-induced mechanical deformation. In fact, common piezoceramic components would not withstand their installation (gluing) on the curved surface of the top foil. Moreover, the attached MFCs do not disturb high strains of the top foil present during operation of the bearing. Finally, the localizations, number and size of the used piezoelectric components result from electrodes accessibility through openings in the bushing, assembly method and wiring guidance options available and geometric limitations.

Characteristics

One of the main drawbacks of MFC application, however, is a relatively high amplitude of voltage that is required to cause visible (i.e., measurable) mechanical response. Additionally, in the proposed solution, the centrally localized bumps of the bump foil support the top foil indirectly, i.e., via 0.3mm-thin MFCs.

In the following, there are presented and discussed the results of the experimental study conducted to assess the effectiveness of application of MFCs to control the GFB's operation.

### 3. PIEZOELECTRIC CONTROL OF GFB'S OPERATION - EXPERIMENTAL RESULTS AND DISCUSSION

Table 2 specifies the authors' assumptions made for the investigated case study and presents the configuration of the utilized test stand. Figure 5 visualizes the temporal courses for the operational parameters of the investigated GFB. The expected electrically–induced periodic step-like changes of the strain measured for the top foil are clearly visible, especially for the highest values of supplied voltage, i.e., 150V and 120V, as marked with black dots in the bottom most plot registered for the arbitrarily selected strain gauge. The values of the electrically-induced strains are presented in Table 3.

Descriptions and remarks

Table 2: Characteristics of the conducted experiment.

Characteristics	Descriptions and remarks	
Support configuration	Floating (a single bearing supporting node) configuration - solely with a tested GFB, the shaft's journal supports the bearing	
Stages of the GFB's operation and rotational speed profile	A single cycle of the following stages of GFB's operation:  • run-up with linear growth of speed up to 24000rpm – lasting for 30s  • stable operation at 24000rpm – for the period of 665s,  • run-out with linear decrease of speed down to 0rpm – lasting for 30s,  • break;	
Voltage supplied to MFCs (voltage profile)	Several various amplitudes of voltages are considered in the temporal plot of its profile: 150V, 120V, 90V, 60V, 30V; For each amplitude, the sequence of voltage activation and deactivation (with step functions) is repeated twice. For all subsequent levels of swapping voltage, their values are maintained for 30s.	
Measured quantities and types of sensors	<ol> <li>Temperature - measured with thermocouples,</li> <li>Strain - measured with strain gauges,</li> <li>Rotational speed - measured with an optical sensor Measurements are conducted with the sensors installed on the top foil.</li> </ol>	
Activation	Activation is performed via voltage-controlled MFCs and used to control the curvature of the top foil	

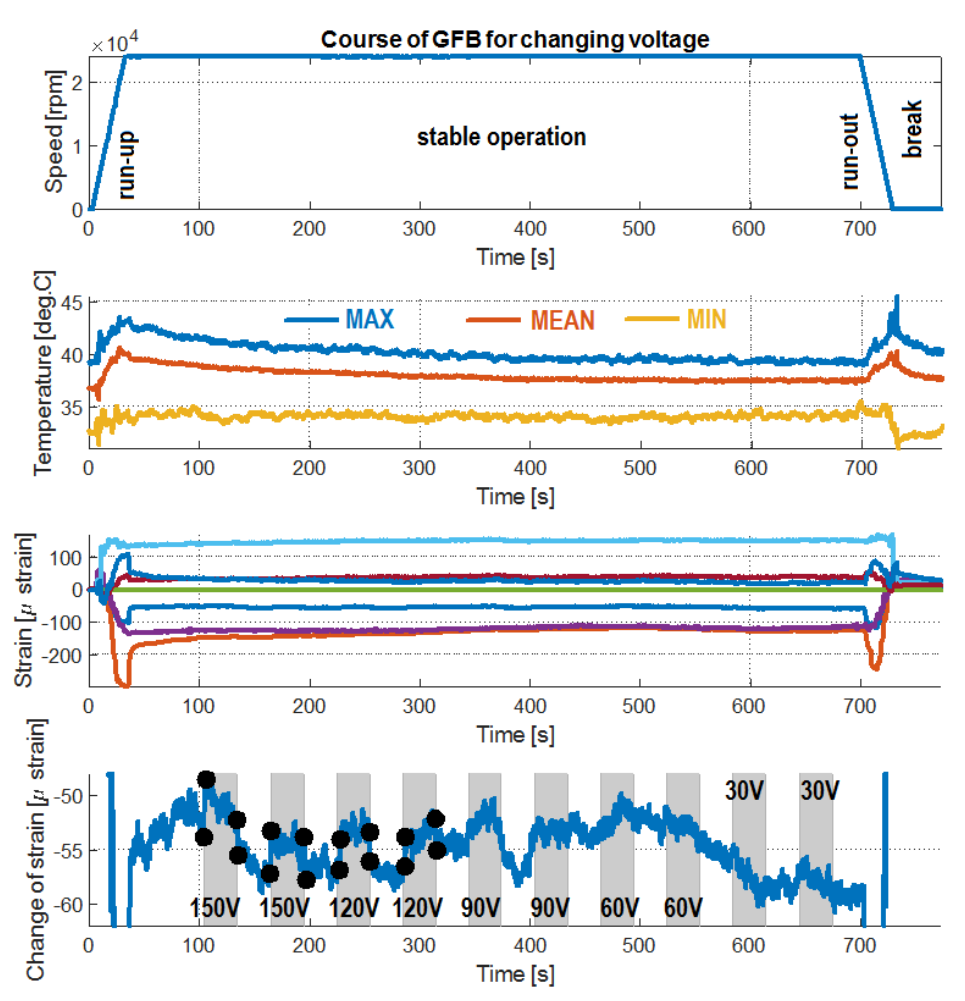


Figure 5: The parameters of the operating GFB

The most bottom plot in Figure 5 represents the registered changes of the strain due to the cyclic voltage swapping, where the strain is measured by the arbitrarily selected strain gauge. The subsequent grey boxes reference to the time intervals exhibiting the continuously decreasing amplitudes of supplied voltage, as stated in Table 2. There are visualized the most significant and, in the authors' opinion, indisputable changes regarding the measured strain found for 150V and 120V electrical activation via piezoelectric components.

Table 3: Electrically-induced strains in the top foil.

Parameter	Value
Changes of the measured strain caused by the 150V activation	5.35 microstrain (turning on the voltage), 3.24 microstrain (power off), 3.88 microstrain (turning on the voltage), 3.93 microstrain (power off);
Statistic characteristics for the absolute change of the strain for the 150V activation	<ul><li>4.10 microstrain (mean value),</li><li>0.89 microstrain (standard deviation);</li></ul>
Changes of the measured strain caused by the 120V activation	<ul><li>2.81 microstrain (turning on the voltage),</li><li>2.69 microstrain (power off),</li><li>2.73 microstrain (turning on the voltage),</li><li>2.88 microstrain (power off);</li></ul>
Statistic characteristics for the absolute change of the strain for the 120V activation	2.78 microstrain (mean value), 0.085 microstrain (standard deviation);

During the run-up and run-out stages of GFB's operation there is registered a typical increase of the bearing's temperature. In fact, while both developing and loss of the air film an adequate presence of a dry friction leads to the increase of heat generation. This process is natural for GFBs, however, the durations of the above-mentioned stages should be sufficiently short not to cause excessive thermal deformations of the bearing's foils that would result in a GFB's damage.

It is worth mentioning that while final break (cooling-down stage) of the GFB, the strains measured by all strain gauges converge do their initial values. Specifically, these strains converge to zero since their offset values were cancelled at the moment of measurement initiation. This observation confirms that the tested GFB operates correctly for the entire experiment course and should be considered typical for the applied floating bearing configuration. As found in the experiment, the GFB's top foil seems to return to its initial position and deformation, after final disappearance of both the hydrodynamic action and thermal expansion.

Moreover, the correct operation of the tested bearing is also confirmed by the continuous decrease of the mean value of the measured temperature within the period of stable operation, i.e., after an initial growth of the above-mentioned parameter during the run-up stage of GFB's operation. Any serious and longer-period instability regarding the characteristics of the thermomechanical coupling observed within the area of air film should inevitably lead to its degradation or even loss of the fluidic component of the supporting layer. Eventually, the evoked dry friction would initiate heat generation followed by a quick rise of the bearing's temperature. Advantageously, no such a behavior was observed by the authors during operation of the investigated prototype, also during cyclic activations of piezoelectric transducers.

As reported in Table 3, activation of piezoelectric composites allows modification of the shape of the top foil. The identified electrically-induced changes of strain are repeatable and may be applied to effectively control the geometry of the several-micrometer-thin air film,

and, hence, influence the operational conditions including the load carrying capacity of the tested bearing. Moreover, as expected, there is also visible a trend of reducing the amplitude of the generated step-like changes of strain as the amplitude of the supplied voltage decreases.

In the authors opinion, a cyclic external electromechanical excitation may advantageously help to adjust and then keep correct the position of the bearings' foils with respect to the shaft's journal – via the small-amplitude mechanical oscillations caused whenever desired in line with the continuously performed temperature readings. However, the above-formulated statement requires farther research to confirm the scope of applicability of the piezoelectric actuation dedicated to the enhancement of the GFB's operational parameters.

#### 4. SUMMARY AND FINAL CONCLUSIONS

In the paper, an application of a novel multifunctional top foil used to modify the properties of the operating GFB's prototype installation (a smart GFB) is presented. Specifically, the developed specialized foil allows for both sensing and actuating operations making use of integrated thermocouples, strain gauges and piezoelectric composites. The former two types of the used sensors enable the bearing's thermomechanical characterization via temperature and strain readings carried out for the top foil. Complementarily, the MFCs are used for electromechanical actuation. The experimental results confirm the usability of the proposed actively-controlled configuration of the GFB. The authors provide the means to achieve repeatable electrically-induced changes of the air film geometry, and, hence, control the operational conditions of the tested bearing.

Having considered the results obtained during the currently reported study, the authors propose the following scope of farther research:

- investigation of the two-support configuration of a GFB making use of the developed multifunctional top foil [5],
- study on the influence of rotational speed and load on the performance of the proposed solution,
- tracking the shaft's journal trajectory during piezoelectric actuation,
- assessment of the vibration reduction capability and estimation of the mechanical energy loss efficiency for the proposed piezoelectric-based solution,
- study on the perspective of energy harvesting making use of the developed specialized top foil;

#### **ACKNOWLEDGEMENTS**

This research was funded by the National Science Center, Poland, within the project grant number 2017/27/B/ST8/01822 entitled "Mechanisms of stability loss in high-speed foil bearings - modeling and experimental validation of thermomechanical couplings".

#### REFERENCES

- [1] Mcauliffe, C. and Dziorny, P.J., Bearing cooling arrangement for air cycle machine. U.S. Patent 5113670, 19 May 1992.
- [2] DellaCorte, C. and Bruckner, R.J., Remaining technical challenges and future plans for oil-free turbomachinery. ASME Journal of Engineering for Gas Turbines and Power, 2011, 133, 042502.

- [3] Samanta, P., Murmu, N.C. and Khonsari, M.M., The evolution of foil bearing technology. Tribology International, 2019, 135, 305–323.
- [4] Gu, Y., Ren, G. and Zhou, M., A fully coupled elastohydrodynamic model for static performance analysis of gas foil bearings. Tribology International, 2020, 147, 106297.
- [5] Martowicz, A., Zdziebko, P., Roemer, J., Zywica, G., and Baginski, P., Thermal characterization of a gas foil bearing a novel method of experimental identification of the temperature field based on integrated thermocouples measurements, Sensors, 2022, 22, 5718.
- [6] Martowicz, A., Roemer, J., Kantor, S., Zdziebko, P., Zywica, G., and Baginski, P., Gas foil bearing technology enhanced with smart materials, Applied Sciences, 2021, 11, 2757.
- [7] Radil, K. and Batcho, Z., A novel thermal management approach for radial foil air bearings, USA Laboratory Report; No. ARL-MR-0749; US Army Research Defense Technical Information Center: Fort Belvoir, VA, USA, 2010.
- [8] San Andres, L., Ryu, K. and Kim, T.H., Thermal management and rotordynamic performance of a hot rotor-gas foil bearings system Part I: Measurements. ASME Journal of Engineering for Gas Turbines and Power, 2011, 133, 062501.
- [9] San Andres, L., Ryu, K. and Kim, T.H., Thermal management and rotordynamic performance of a hot rotor-gas foil bearings system Part II: Predictions versus test data. ASME Journal of Engineering for Gas Turbines and Power, 2011, 133, 062502.
- [10] Feng, K., Cao, Y., Yu, K., Guan, H.-Q., Wu, Y. and Guo, Z., Characterization of a controllable stiffness foil bearing with shape memory alloy springs. Tribology International 2019, 136, 360–371.
- [11] Nielsen, B.B., Combining gas bearing and smart material technologies for improved machine performance theory and experiment. Ph.D. Thesis, Technical University of Denmark, Kongens Lyngby, Denmark, 2017; No. S221.
- [12] Nielsen, B.B., Nielsen, M.S. and Santos, I.F., A layered shell containing patches of piezoelectric fibers and interdigitated electrodes: Finite element modeling and experimental validation. Journal of Intelligent Material Systems and Structures, 2016, 28, 78–96.
- [13] Sadri, H., Kyriazis, A., Schlums, H. and Sinapius, M., On modeling the static shape control of an adaptive air foil bearing. Smart Materials and Structures, 2020, 29, 085043.
- [14] Ghalayini, I. and Bonello, P., Nonlinear and linearised analyses of a generic rotor on single-pad foil-air bearings using Galerkin Reduction with different applied air film conditions. Journal of Sound and Vibration, 2022, 525, 116774.
- [15] Feng, K., Guan, H.-Q., Zhao, Z.-L. and Liu, T.-Y., Active bump-type foil bearing with controllable mechanical preloads. Tribology International, 2018, 120, 187–202.
- [16] Guan, H.Q., Feng, K., Yu, K., Cao, Y.L. and Wu, Y.H. Nonlinear dynamic responses of a rigid rotor supported by active bump-type foil bearings. Nonlinear Dynamics, 2020, 100, 2241–2264.
- [17] Guan, H.Q., Feng, K., Cao, Y.L., Huang, M., Wu, Y.H. and Guo, Z.Y., Experimental and theoretical investigation of rotordynamic characteristics of a rigid rotor supported by an active bump-type foil bearing. Journal of Sound and Vibration, 2020, 466, 115049.
- [18] Polyakov, R., Bondarenko, M. and Savin, L., Hybrid bearing with actively adjustable radial gap of gas foil bearing. Procedia Engineering, 2015, 106, 132–140.

- [19] Wang, E., Gardner, N., Gupta, S. and Shukla, A., Fluid-structure interaction and its effect on the performance of composite structures under air-blast loading. The International Journal of Multiphysics, 2012, 6(3), 219-240.
- [20] Kwon, Y., Owens, A. and Kwon, A., Experimental Study of Impact on Composite Plates with Fluid-Structure Interaction. The International Journal of Multiphysics, 2010, 4(3), 259-271.
- [21] Andleeb, Z., Malik, S., Khawaja, H., Antonsen, S., Hassan, T., Hussain, G. and Moatamedi, M., Strain Wave Analysis in Carbon-Fiber-Reinforced Composites subjected to Drop Weight Impact Test using ANSYS®. The International Journal of Multiphysics, 2021, 15(3), 275-290.
- [22] Afzali, M. and Rostamiyan, Y., Study the damping and vibrational properties of polycarbonate reinforced ZrO2. The International Journal of Multiphysics, 2022, 16(1), 31-52.
- [23] Mezdour, D., Sahli, S. and Tabellout, M., Study of the electrical conductivity in fiber composites. The International Journal of Multiphysics, 2010, 4(2), 141-150.
- [24] Roemer, J., Zdziebko, P. and Martowicz, A., Multifunctional bushing for gas foil bearing test rig architecture and functionalities. The International Journal of Multiphysics, 2021, 15(1), 73-86.
- [25] Smart Material Corporation, https://www.smart-material.com/MFC-product-P1V2.html
- [26] Acciani, G., Dimucci, A. and Lorusso, L., Multimodal piezoelectric devices optimization for energy harvesting. The International Journal of Multiphysics, 2013, 7(3), 227-244.
- [27] Martowicz, A., Rosiek, M., Manka, M. and Uhl, T., Design Process of IDT Aided by Multiphysics FE Analyses. The International Journal of Multiphysics, 2012, 6(2), 129-148.